

Title: Effect of a collar on subsidence and local micromotion of cementless femoral stems: in vitro comparative study based on micro-CT

Running title: Collar effect on stem stability

Author 1

Valérie Malfroy Camine
Final degree(s): MSc
Laboratory of Biomechanical Orthopedics
Ecole Polytechnique Fédérale de Lausanne
Station 19
1015 Lausanne
Switzerland
Email: valerie.malfroycamine@epfl.ch

Author 2

Hannes A. Rüdiger
Final degree(s): MD
Department of Orthopedic Surgery
Schulthess Clinic
Lengghalde 2
8008 Zürich
Switzerland

Service of Orthopedics and Traumatology
Lausanne University Hospital
Avenue Pierre Decker 4
1011 Lausanne
Switzerland
Email: hannes.ruediger@kws.ch

Author 3

Dominique P. Pioletti
Final degree(s): PhD
Laboratory of Biomechanical Orthopedics
Ecole Polytechnique Fédérale de Lausanne
Station 19
1015 Lausanne
Switzerland
Email: dominique.pioletti@epfl.ch

Author 4

* Corresponding author:
Alexandre Terrier
Final degree(s): PhD
Laboratory of Biomechanical Orthopedics

Ecole Polytechnique Fédérale de Lausanne
Station 19
1015 Lausanne
Switzerland
Email: alexandre.terrier@epfl.ch

Word count: 2911

Keywords: Collar; Primary stability; Micromotion; Subsidence; Femoral stem; Cementless Total Hip Arthroplasty

Acknowledgements

This work has been supported by Swiss National Science Foundation (#141152) and the SwissLife Jubiläumstiftung. The authors thank DePuy Synthes (DePuy Synthes Joint Reconstruction, Warsaw, IN, USA) for providing the implants, instruments and CAD files, and Alejandro Dominguez and the Centre Universitaire Romand de Médecine Légale (CURML) for the CT-scans of the femurs.

Conflict of Interest Statement

This study was founded by the Swiss National Science Foundation (#141152) and by the SwissLife Jubiläumstiftung. The funding source did not play a role in the investigation. Each author certifies that he or she, or a member of his or her immediate family, has no funding or commercial associations (e.g. consultancies, stock ownership, equity interest, patent/licensing arrangements, etc.) that might pose a conflict of interest in connection with the submitted article.

Ethical Review Committee Statement

Each author certifies that his or her institution approved or waived approval for the human protocol for this investigation and that all investigations were conducted in conformity with ethical principles of research. This study was performed in accordance with the ethical standards in the 1964 Declaration of Helsinki. The local ethical committee approval is not required for biomechanical test on human cadaveric bones.

This work was performed at the Ecole Polytechnique Fédérale de Lausanne and the Centre Hospitalier Universitaire Vaudois, Lausanne, Switzerland.

1 **Abstract**

2 *Purpose* The aim of this study is to quantitatively compare the difference in primary stability
3 between collarless and collared versions of the same femoral stem. Specifically, we tested
4 differences in subsidence and micromotion.

5 *Methods* Collarless and collared versions of the same cementless femoral stem were implanted in
6 two groups of six fresh-frozen cadaveric femurs. Each implanted femur was then subsequently
7 tested for axial compressive and torsional loadings. A micro-CT based technique was applied to
8 quantify implant subsidence and compute the map of local micromotion around the femoral
9 stems. Micromotion of collarless and collared stems was compared in each Gruen zone.

10 *Results* Subsidence was higher but not significantly ($p = 0.352$) with collarless ($41.0 \pm 29.9 \mu\text{m}$)
11 than with collared stems ($37.0 \pm 44.6 \mu\text{m}$). In compression, micromotion was lower ($p = 0.257$)
12 with collarless ($19.5 \pm 5 \mu\text{m}$) than with collared stems ($43.3 \pm 33.1 \mu\text{m}$). In torsion, micromotion
13 was also lower ($p = 0.476$) with collarless ($96.9 \pm 59.8 \mu\text{m}$) than collared stems (118.7 ± 45.0
14 μm). Micromotion was only significantly lower ($p = 0.001$) in Gruen zone 1 and for compression
15 with collarless ($7.0 \pm 0.6 \mu\text{m}$) than with collared stems ($22.6 \pm 25.5 \mu\text{m}$).

16 *Conclusions* Primary stability was achieved for both stem designs, with a mean micromotion
17 below the osseointegration threshold. Under loading conditions similar to those observed in
18 normal daily activity and with good press-fit, the collar had no influence on subsidence or
19 micromotion. Further studies are required to test the potential advantage of collar with higher
20 loads, undersized stems, or osteoporotic femurs.

21 **Introduction**

22 Anchorage of cementless implants in bone is achieved through osseointegration, i.e. the direct
23 mechanical interlock that forms between the host bone and the implant surface. The primary
24 stability of the implant (the stability of the implant directly after the operation) is essential for a
25 successful osseointegration. The primary stability is characterized by the relative motion between
26 the bone and the implant that takes place when the implant is loaded, and multiple studies have
27 shown that excessive amounts of implant micromotion prevent osseointegration [1, 2].

28 Since the introduction of cementless total hip arthroplasty (THA) in the late 1950s, many design
29 modifications have been proposed to improve the primary stability and long-term survival of
30 femoral stems [3, 4]. Collared designs are thought to enhance primary stability and hence
31 osseointegration by improving resistance to axial, rotational, and varus forces at the bone implant
32 interface [4]. This might be of importance in view of the current trend to allow for early weight
33 bearing after total hip arthroplasty. However, the use of collared designs is controversial, as
34 concerns in regards to their downsides have been raised [3]. For an optimal load transmission, a
35 perfect contact between the collar and the calcar is a mandatory prerequisite. This necessitates
36 additional surgical steps and surgical time. In addition, the presence of a collar may prevent the
37 full settling of the stem in the medullary canal. Finally, a collar may complicate extraction when
38 removal of an integrated stem becomes necessary.

39 Clinical studies have reported no difference in the revision rate of collarless and collared
40 versions of the same stem [3]. In contrast, Demey *et al.* [4] reported that a collar increased the
41 force required to initiate implant subsidence and intraoperative periprosthetic fractures.

42 Primary stability is characterized by interfacial bone-implant micromotion. A good primary
43 implant stability is associated with low micromotion, and is critical for osseointegration and
44 hence long-term success of THA. Nevertheless, quantitative data on the differences in primary
45 stability between collarless and collared stems are scarce, and the available studies are based on
46 finite-element models, which were not validated experimentally [5, 6].

47 The purpose of this study was to determine the difference in primary stability between collarless
48 and collared versions of the same femoral stem. Specifically, we asked the following questions:
49 (1) Does a collar prevent stem subsidence? (2) Is there a difference in local micromotion around
50 collarless and collared designs during compressive and (3) torsional loadings? A novel *in vitro*
51 technique providing the complete map of local micromotion on the intramedullary surface of
52 femoral stems [7–9] was used.

Materials and Methods

Twelve fresh-frozen human cadaveric femurs (National Disease Research Interchange, Philadelphia, PA, USA) were wrapped in saline-soaked gauze, placed in airtight plastic bags and stored at -70 °C immediately after dissection. The selection criteria excluded femurs of individuals with a history of radiation or malignant disease, or previous femoral fractures. There were three females and nine males. Mean age was 71 years (32 - 93 years, mean weight 83 kg (56 – 143 kg), and mean BMI 29 kg/m² (18.3 - 47.8 kg/m²). Detailed information about donors and implants can be found in supplementary material (Electronic Supplementary Material 1).

Specimens were thawed at room temperature in saline solution and remaining soft tissues were removed. Femoral neck was cut and compaction broaching were performed by a senior orthopedic surgeon following manufacturer's recommendations using the original instrumentation. The proximal metaphyseal bone was compacted using the bone tamp. The broaches were then impacted in increasing sizes manually with a hammer until axial stability was achieved. Then, rotational stability was tested by turning the broach handle manually clock and counter-clock wise. The stem was considered clinically stable when no macroscopic movement at the bone-implant interface could be observed. Around 1000 stainless steel spherical markers (diameter 600 µm, MPS Micro Precision Systems AG, Biel, Switzerland) were manually press-fitted in the metaphyseal cancellous bone and on the endosteal surface of the femoral canal using a spatula.

Six collarless and six collared versions of the same cementless femoral stem (Corail® Hip System, DePuy Synthes Joint Reconstruction, Warsaw, IN, USA) were selected for implantation. The stem is made of forged titanium alloy (TiAl6V4), and is fully coated with 155 µm of

hydroxyapatite. Thirty-seven tantalum spherical markers (diameter 800 μm , X-medics Scandinavia, Frederiksberg, Denmark) were glued (Loctite 401, Loctite 55 Corporation, Dublin, Ireland) uniformly on the stem surface, within drilled holes of 1 mm depth and 850 μm diameter. Due to the limited size of the micro-CT scanner, the femoral necks of the stems were cut 27 mm medial and parallel to the implant extraction threaded hole axis. Femoral stems were then implanted, and the femurs were wrapped in saline-soaked gauze, placed in airtight plastic bags and stored again at $-70\text{ }^{\circ}\text{C}$.

All femurs were successively tested for axial compression and torsion using two separate loading devices, designed to fit inside a Skyscan 1076 micro-CT scanner (Bruker micro-CT, Kontich, Belgium) (Fig. 1) The acquisition parameters for the scans were the following: 1 mm aluminum filter, voltage 100 kV, current 100 μA , exposure time 310 ms, rotation step 0.7° , 360° scanning, scanning width 68 mm, and frame averaging 2. The scanning length was 21 mm. To cover the whole implant length, 7 scans at different positions along the stem were combined by moving the motorized sample's stage accordingly. Scanning duration for one 21 mm scan was 24 min, resulting in 170 min of scanning to cover the whole stem. Scans were then reconstructed to a final isotropic voxel size of 35 μm (NRecon v 1.6.10.4, Bruker micro-CT, Kontich, Belgium). A ring artifact correction of level 4 and a beam hardening correction of 20% were applied to improve the image quality. The maximum bias of the method was 5.1 μm . The bias was consistent between directions as well as between loading cases [9]. Subsidence was defined as the irreversible vertical migration of the implant after loading, while local micromotion was defined as the reversible elastic motion of the stem during loading. Before testing, femurs were thawed at room temperature, and kept humid with saline-soaked gauze during all subsequent preparation and testing steps.

For compression testing, the distal part of each femur was potted in epoxy resin 30 mm distal of the tip of the stem. For each femur, a load corresponding to 230% of donor's body weight (BW) was applied on the shoulder of the stem, aligned with the stem extraction threaded hole axis. Compression testing was uniaxial. The load was chosen according to the average load during walking measured with instrumented hip implants [10]. The applied load was static. Before testing, bone was pre-conditioned with 10 successive compressive loads, to enable full settling of the stem in the bone cavity. Pre-conditioning was performed with the same load as for testing. The displacement rate and duration of unloaded phases were not controlled, load was applied and removed manually.

For torsion testing, femurs were again potted distally with epoxy resin and a clamping system was used to restrain the proximal stem. For each femur, a moment corresponding to $2.3\% \text{ BW} \times \text{m}$ was applied around the stem extraction threaded hole axis (internal rotation of the stem). The load was chosen according to the average moment during stair climbing measured with instrumented hip implants [10]. Before testing, the bone was pre-conditioned with 10 successive torsional loads.

To measure implant subsidence and local micromotion in compression, three successive micro-CT scans of the whole bone-implant interface were performed: the first scan was performed without load and represented the initial state before pre-conditioning of the bone, the second scan was performed while compressive load was applied, and the third scan was performed after the compressive load had been removed. Bone and implant markers were then automatically segmented on the reconstructed images, and the three scans were rigidly registered based on implant markers positions to align all scans in the same coordinate system. Subsidence was calculated as the mean vertical displacement of corresponding bone markers between the initial

unloaded scan and the final unloaded scan. Local micromotion was obtained from the 3D displacement vector between corresponding bone markers in the loaded scan and the final unloaded scan (Fig. 2). The same method was applied for torsion.

Two femurs in the collarless had to be excluded. One femur was excluded due to a periprosthetic fracture during compressive loading. Another femur had to be excluded because measurement data were unusable after a failure of the imaging system.

All data analysis was carried out in MATLAB (Matlab r2016a, The Mathworks, Inc., Natick, MA, USA). The micromotion vector was calculated at each point and its absolute value (i.e. magnitude) in micrometers was determined. The micromotion vector was further divided into its tangential and normal components, relative to the stem surface. Natural-neighbor interpolation between all measurement points was used to create maps of micromotion on each stem's surface.

The femoral stems were divided into 12 zones corresponding to Gruen zones 1 to 3, 5 to 10, and 12 to 14 [11]. To investigate the relationship between median micromotion or median subsidence, and donor's age, weight, BMI, and implant size, the Spearman's rank correlation coefficient was evaluated and its significance was assessed using a permutation test. A Mann-Whitney U-test was chosen to compare collarless and collared stems subsidence, because this test does not make assumptions about homogeneity of variances or normal distributions of the data. The same Mann-Whitney U-test was used to compare median micromotion between collarless and collared stems in each Gruen zone. The significance level for all statistical tests performed was set to 0.05.

Results

Mean stem subsidence did not differ significantly between the two groups ($41.0 \mu\text{m} \pm 29.9 \mu\text{m}$ and $37.0 \mu\text{m} \pm 44.6 \mu\text{m}$ in the collarless and collared group, respectively ($p=0.352$)).

Between 213 and 432 simultaneous measurement points uniformly distributed around each implant were obtained, resulting in full-field maps of micromotion around the stems for compressive and torsional loads (Fig. 3). In compression, mean absolute micromotion was $19.5 \mu\text{m} \pm 5 \mu\text{m}$ in the collarless group and $43.3 \mu\text{m} \pm 33.1 \mu\text{m}$ in the collared group ($p = 0.257$). The only significant local difference between the collarless and the collared group occurred for absolute micromotion in Gruen zone 1 ($p = 0.01$), with a mean absolute micromotion of $7.0 \mu\text{m} \pm 0.6 \mu\text{m}$ for the collarless group and $22.6 \mu\text{m} \pm 25.5 \mu\text{m}$ for the collared group (Fig. 4). No significant difference was detected between the collarless and collared groups, for absolute micromotion, normal micromotion, and tangential micromotion (Electronic Supplementary Material 3). For both stem designs, micromotion was lower, but not significantly (Electronic Supplementary Material 3), around the proximal part of the stem (Gruen zones 1, 7, 8 and 14) and higher distally.

In torsion, absolute micromotion was higher than in compression, with a mean of $96.9 \mu\text{m} \pm 59.8 \mu\text{m}$ in the collarless group and $118.7 \mu\text{m} \pm 45.0 \mu\text{m}$ in the collared group ($p = 0.476$). No significant difference was found between collarless and collared stems, for absolute micromotion, normal micromotion, and tangential micromotion (Fig. 5 and Electronic Supplementary Material 3).

There was no significant correlation between patient's age, weight, BMI or implant size, and stem subsidence or micromotion ($p>0.05$) (Electronic Supplementary Material 2). For all stems,

163 mean micromotion was 37.4 μm in compression and 119.9 μm in torsion. One of the femur in
164 the collared group presented with much higher stem micromotion in torsion than the rest of the
165 femurs. For this femur, mean micromotion in torsion was 252.9 μm and micromotion reached a
166 maximum of 625.9 μm locally, in Gruen zone 1.

Discussion

The primary stability of femoral stems is essential for the long-term success of cementless total hip arthroplasty. Low micromotion is a prerequisite for osseointegration of the implant and limits the formation of interfacial fibrous tissue [1, 2]. Collared stems in cementless THA are gaining increasing popularity based on the hypothesis that they enhance implant primary stability, or that a progression of unrecognized fissures occurring during surgery may be prevented by a collar, particularly in presence of poor bone quality. However, there is only limited evidence to support this hypothesis. Clinical studies did not show any significant benefit of collared stems in terms of implant survival [12, 13]. Biomechanical studies were limited to finite element modeling [5, 6], which are insufficiently backed by experimental data. Our objective was to determine if there is a significant difference in primary stability between collarless and collared stems, by measuring subsidence and local micromotion around collarless and collared stems in cadaveric femurs, using a previously described micro-CT based *in vitro* technique. The most important finding of this study was that no significant difference was detected between collarless and collared designs, in terms of subsidence or local micromotion, except for a small variation in micromotion in Gruen zone 1 in compression.

The absence of significant difference in subsidence between collarless and collared stems is consistent with the work of Meding *et al.* [13], reporting no difference in subsidence in a prospective randomized study that compared identical cementless stems with and without collar up to 5 years postoperatively. Demey *et al.* [4] demonstrated in a cadaveric study that collared designs required a significantly higher force to initiate subsidence of the stem and to cause a periprosthetic fracture than collarless stems. However, the force necessary to initiate subsidence of the stem was superior to 3000 N for both groups, which is a much higher load than those

experienced during activities of daily living. Such high loads might only be encountered in heavy patients or during high impact activities or falls [14].

Our measurements of micromotion during compression and torsion are in general agreement with previous reports [15, 16]. For all stems, mean micromotion was 37.4 μm in compression and 119.9 μm in torsion, which is below the reported maximum threshold allowing osseointegration ($<150 \mu\text{m}$) [17, 18]. This result suggests that a satisfactory primary stability was achieved, regardless of the presence or absence of a collar. Our observation that in general micromotion is higher in torsion than in compression, was also reported by several authors [19–21]. The technique we used to measure local micromotion, based on micro-CT imaging, offers a novel understanding of the biomechanics behind cementless stems primary stability. The absence of significant difference in local micromotion between collarless and collared in most Gruen zones is in line with clinical studies indicating similar revision rates for both types of implants [12, 21]. This result suggests that there is no significant difference in primary stability between collarless and collared implants. We observed significantly higher absolute micromotion for collared stems in Gruen zone 1 for compressive but not for torsional loading. However, this difference was small (15 μm), and in view of the results in all other Gruen zones for both types of loading, it seems unlikely that collars are associated with a relevant decrease in primary stability.

Of note, we observed a periprosthetic fracture in one of the specimen implanted with a collarless implant during compressive loading. Despite that some authors reported that collarless stems are at a higher risk of periprosthetic fractures than collared stems [4], we don't think that the fracture in this specimen can be conclusively attributed to the collarless design. Indeed, we adapted the

load to the donor's body weight, and this resulted for this overweight donor in an extreme load of over 3200N, which we believe explains the fracture.

There are a number of weaknesses in this study. First, the sample size in this technically demanding study is small and anatomy and bone quality vary among the samples. Due to the limited sample size we did not further characterize or classify the femoral anatomy, as comparisons among subgroups would not have been possible. The unbalanced sex-ratio is also not representative of the actual patient population in cementless hip arthroplasty. The implantation of the stems into dissected cadaveric femurs is facilitated by the absence of soft tissue and a strong press-fit was achieved in all cases, not necessarily reflecting the clinical setting. Indeed, impingement phenomena occur under physiological conditions and may influence the subsidence or micromotion of the stem. The loading protocol used in this study separated axial compressive load and axial torsional load. Consequently, the results may have been partially affected by the fact that these loadings are not physiological. The loads applied in this work correspond to those encountered during activities of daily living under full weight bearing. Higher loads (e.g. during stumbling or in obese patients) may lead to different results. Finally, owing to the complexity of the experimental protocol, multiple thawing and freezing cycles of the femurs were necessary. In order to preserve the mechanical properties of bone, all freezing and thawing steps were performed within saline solution and the bones were kept humid at all times in between. Previous research showed that multiple freezing and thawing of fresh frozen bone did not affect the specimen's mechanical properties when the above precautions were strictly applied [22, 23].

In conclusion, we did not observe differences in primary stability (subsidence and micromotion) between collarless and collared stems, within the limitations of *in vitro* measurements partly

235 replicating activities of daily living. This finding could be beneficial to help surgeons decide
236 between a collarless or a collared implant, as no consensus on this question has been reached yet.
237 Further studies remain necessary to investigate whether collars may be advantageous in the
238 presence of higher loads, undersized stems, or for decreased or increased bone densities or
239 anatomical variants (e.g. varus or valgus necks).

References

1. Jasty M, Bragdon CR, Zalenski E, et al (1997) Enhanced stability of uncemented canine femoral components by bone ingrowth into the porous coatings. *J Arthroplasty* 12:106–113. doi: 10.1016/S0883-5403(97)90055-3
2. Soballe K, Hansen ES, H B-R, et al (1992) Tissue ingrowth into titanium and hydroxyapatite-coated implants during stable and unstable mechanical conditions. *J Orthop Res* 10:285–99.
3. Hutt J, Hazlerigg A, Aneel A, et al (2014) The effect of a collar and surface finish on cemented femoral stems: A prospective randomised trial of four stem designs. *Int Orthop* 38:1131–1137. doi: 10.1007/s00264-013-2256-z
4. Demey G, Fary C, Lustig S, et al (2011) Does a Collar Improve the Immediate Stability of Uncemented Femoral Hip Stems in Total Hip Arthroplasty? A Bilateral Comparative Cadaver Study. *J Arthroplasty* 26:1549–1555. doi: 10.1016/j.arth.2011.03.030
5. Ebramzadeh E, Sangiorgio SN, Longjohn DB, et al (2004) Initial stability of cemented femoral stems as a function of surface finish, collar, and stem size. *J Bone Jt Surg Am* 86–A:106–15.
6. Mandell JA, Carter DR, Goodman SB, et al (2004) A conical-collared intramedullary stem can improve stress transfer and limit micromotion. *Clin Biomech* 19:695–703. doi: 10.1016/j.clinbiomech.2004.04.004
7. Gortchacow M, Wettstein M, Pioletti DP, Terrier A (2011) A new technique to measure micromotion distribution around a cementless femoral stem. *J Biomech* 44:557–60. doi: 10.1016/j.jbiomech.2010.09.023
8. Gortchacow M, Wettstein M, Pioletti DP, et al (2012) Simultaneous and multisite measure of micromotion, subsidence and gap to evaluate femoral stem stability. *J Biomech*. doi: 10.1016/j.jbiomech.2012.01.040
9. Malfroy Camine V, Rüdiger HA, Pioletti DP, Terrier A (2016) Full-field measurement of micromotion around a cementless femoral stem using micro-CT imaging and radiopaque markers. *J Biomech* 49:4002–4008. doi: 10.1016/j.jbiomech.2016.10.029
10. Bergmann G, Graichen F, Rohlmann A, et al (2010) Realistic loads for testing hip implants. *Biomed Mater Eng* 20:65–75. doi: 10.3233/BME-2010-0616
11. Gruen TA, McNeice GM, Amstutz HC (1979) “Modes of failure” of cemented stem-type femoral components: a radiographic analysis of loosening. *Clin Orthop* 17–27.
12. Jameson SS, Baker PN, Mason J, et al (2013) Independent predictors of failure up to 7.5 years after 35 386 single-brand cementless total hip replacements: A

- 276 retrospective cohort study using National Joint Registry data. *Bone Jt J* 95 B:747–
277 757. doi: 10.1302/0301-620X.95B6.31378
- 278 13. Meding JB, Ritter MA, Keating EM, Faris PM (1997) Comparison of collared and
279 collarless femoral components in primary uncemented total hip arthroplasty. *J*
280 *Arthroplasty* 12:273–280. doi: 10.1016/S0883-5403(97)90023-1
- 281 14. Bergmann G, Bender A, Dymke J, et al (2016) Standardized loads acting in hip
282 implants. *PLoS ONE*. doi: 10.1371/journal.pone.0155612
- 283 15. Bieger R, Ignatius A, Decking R, et al (2012) Primary stability and strain distribution
284 of cementless hip stems as a function of implant design. *Clin Biomech* 27:158–164.
285 doi: 10.1016/j.clinbiomech.2011.08.004
- 286 16. Fottner A, Peter CV, Schmidutz F, et al (2011) Biomechanical evaluation of
287 different offset versions of a cementless hip prosthesis by 3-dimensional
288 measurement of micromotions. *Clin Biomech* 26:830–835. doi:
289 10.1016/j.clinbiomech.2011.04.001
- 290 17. Engh CA, O'Connor D, Jasty M, et al (1992) Quantification of implant micromotion,
291 strain shielding, and bone resorption with porous-coated anatomic medullary
292 locking femoral prostheses. *Clin Orthop Relat Res* 13–29.
- 293 18. Pilliar RM, Lee JM, Maniopoulos C (1986) Observations on the effect of
294 movement on bone ingrowth into porous-surfaced implants. *Clin Orthop Relat Res*
295 108–13.
- 296 19. Enoksen CH, Gjerdet NR, Klaksvik J, et al (2014) Initial stability of an uncemented
297 femoral stem with modular necks. An experimental study in human cadaver
298 femurs. *Clin Biomech* 29:330–335. doi: 10.1016/j.clinbiomech.2013.12.011
- 299 20. Kassi J-P, Heller MO, Stoeckle U, et al (2005) Stair climbing is more critical than
300 walking in pre-clinical assessment of primary stability in cementless THA in vitro. *J*
301 *Biomech* 38:1143–1154. doi: 10.1016/j.jbiomech.2004.05.023
- 302 21. Østbyhaug PO, Klaksvik J, Romundstad P, Aamodt A (2010) Primary stability of
303 custom and anatomical uncemented femoral stems. *Clin Biomech* 25:318–324. doi:
304 10.1016/j.clinbiomech.2009.12.012
- 305 22. Kang Q, An YH, Friedman RJ (1997) Effects of multiple freezing-thawing cycles on
306 ultimate indentation load and stiffness of bovine cancellous bone. *Am J Vet Res*
307 58:1171–1173.
- 308 23. Linde F, Sørensen HCF (1993) The effect of different storage methods on the
309 mechanical properties of trabecular bone. *J Biomech* 26:1249–1252. doi:
310 10.1016/0021-9290(93)90072-M

Legends

Fig. 1 Loading devices designed to fit inside the micro-CT scanner. (a) Axial compression loading device. The distal femur is cemented and compression is applied through a cylinder driven by a screw jack. (b) Axial torsion loading device. The proximal stem is restrained by a clamping system. The proximal stem and the distal femur are cemented. Torsion is applied through a worm gear.

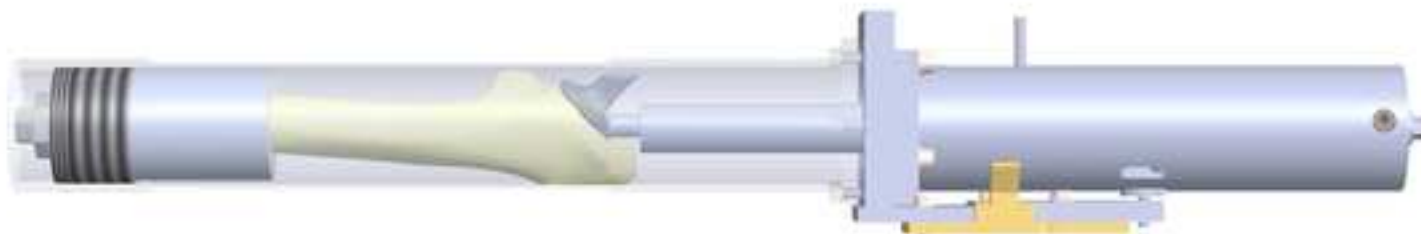
Fig. 2 Subsidence and micromotion computation. Three successive scans are performed, an initial unloaded scan, a loaded scan, and a final unloaded scan. The scans are aligned in the same coordinate system using rigid registration of implant markers. Subsidence is the displacement of corresponding bone markers from the registered initial unloaded scan to the final unloaded scan. Micromotion is the displacement of corresponding bone markers from the registered loaded scan to the final unloaded scan.

Fig. 3 Sample distribution of absolute micromotion around one collarless stem and one collared stem - Anterior/lateral and posterior/medial views of the stem displayed successively from left to right for each case. Top row shows results obtained in compression. The bottom row shows results obtained in torsion.

Fig. 4 Distribution of absolute, normal, and tangential micromotion in compression by Gruen zone around collarless (n=4) and collared (n=6) stems. Box plots show median value (light grey line), 1st and 3rd quartiles (bottom and top of the box), and minimum and maximum values (whiskers). Star (*) indicates significant difference between pairs of distributions (p -value<0.05) using Mann-Whitney U test.

333 **Fig. 5** Distribution of absolute, normal, and tangential micromotion in torsion by Gruen zone
334 around collarless (n=4) and collared (n=6) stems. Box plots show median value (light grey line),
335 1st and 3rd quartiles (bottom and top of the box), and minimum and maximum values (whiskers).

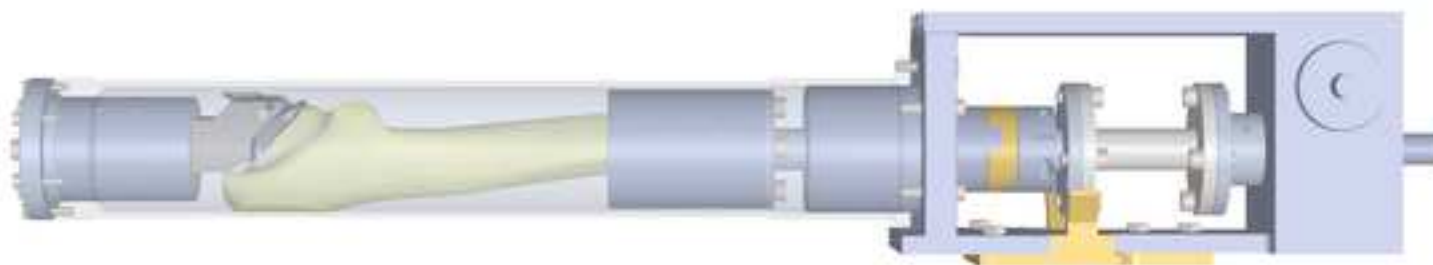
(a)



Axial Compression



(b)



Axial Torsion



Figure 2

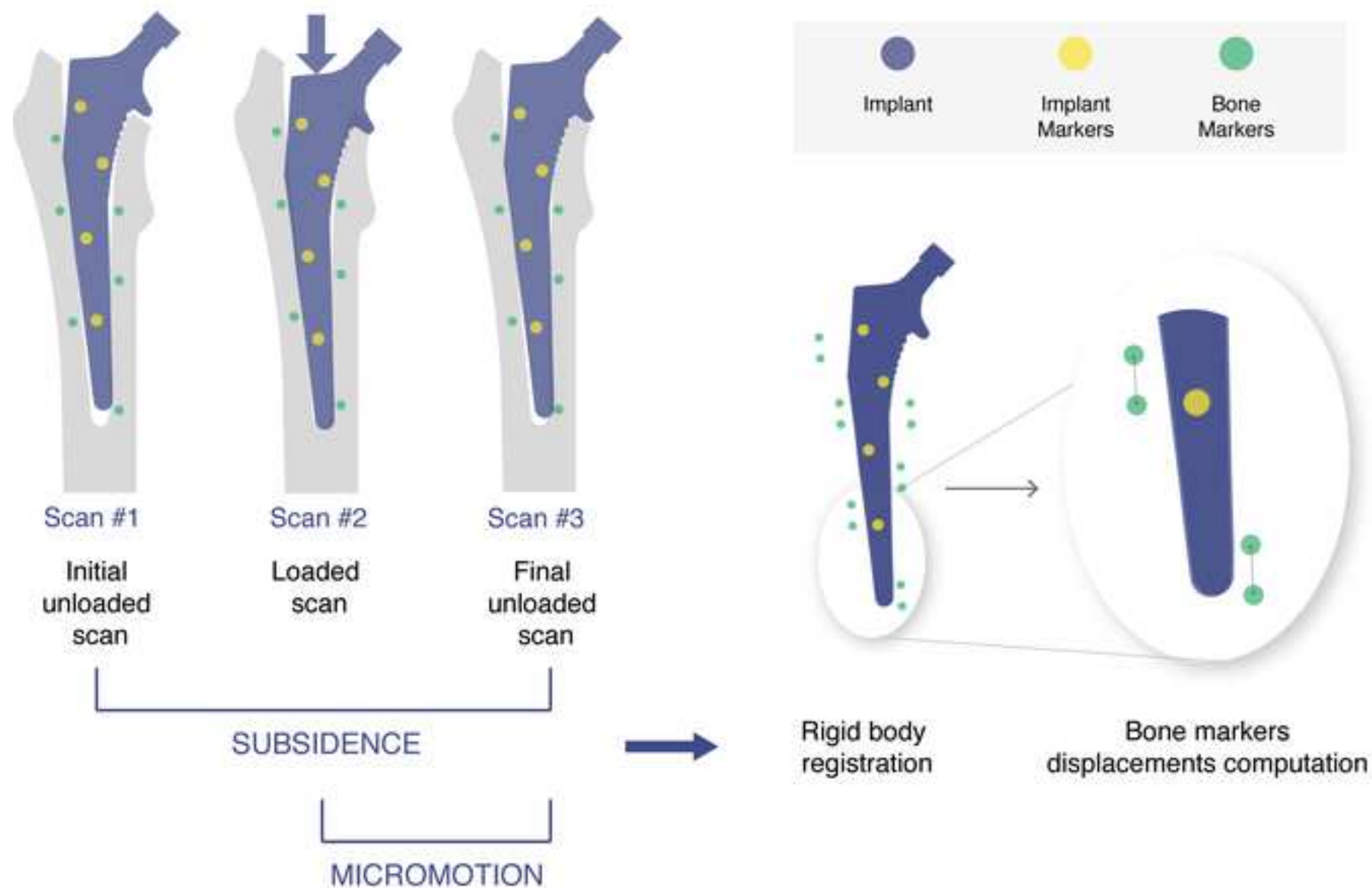


Figure 3

